THE ASTRONOMICAL JOURNAL, 123:1013–1022, 2002 February

ABSOLUTE PROPERTIES OF THE MAIN-SEQUENCE ECLIPSING BINARY STAR WW CAMELOPARDALIS[1]

CLAUD H. SANDBERG LACY[2,3]
Department of Physics, University of Arkansas, Fayetteville, AR 72701; clacy@uark.edu

GUILLERMO TORRES
Harvard-Smithsonian Center for Astrophysics, 60 Garden Street, Cambridge, MA 02138; gtorres@cfa.harvard.edu

ANTONIO CLARET
Instituto de Astrofisica de Andalucía, CSIC, Apartado 3004, E-18080 Granada, Spain; claret@iaa.es

AND

JEFFREY A. SABBY[3]
Department of Physics, University of Arkansas, Fayetteville, AR 72701; jsabby@uark.edu
Received 2001 September 28; accepted 2001 November 14

ABSTRACT

We present absolute photometric observations in $uvby\beta$ and 5759 differential observations in the V filter (the most complete light curve ever obtained) measured by a robotic telescope, as well as radial velocities from spectroscopic observations of the detached, eccentric, 2.3 day, double-lined, eclipsing binary star WW Camelopardalis. Absolute dimensions of the components are determined with high precision (better than 1% in the masses and radii) for the purpose of testing various aspects of theoretical modeling. We obtain $1.920 \pm 0.013\ M_\odot$ and $1.911 \pm 0.016\ R_\odot$ for the primary, and $1.873 \pm 0.018\ M_\odot$ and $1.808 \pm 0.014\ R_\odot$ for the secondary. The effective temperatures and interstellar reddening of the stars are accurately determined from new $uvby\beta$ photometry: 8350 ± 135 K for the primary and 8240 ± 135 K for the secondary, corresponding to a spectral type of A4m for both, and 0.294 mag for E_{b-y}. The metallic-lined character of the stars is revealed by high-resolution spectroscopy and $uvby\beta$ photometry. Spectral line widths give rotational velocities that are synchronous with the orbital motion in a slightly eccentric orbit ($e = 0.0098$). The components of WW Cam are main-sequence stars with an age of about 490 Myr according to models.

Key words: binaries: eclipsing — binaries: spectroscopic — stars: evolution — stars: fundamental parameters — stars: individual (WW Camelopardalis)

On-line material: machine-readable table

1. INTRODUCTION

The discovery of WW Camelopardalis (=DM Cas = BD +64°454, Tycho 4073-1191-1, GSC 04073-01191; V = 10.14–10.84, A4m + A4m V) as an eclipsing binary star is due to Huruhata & Gaposchkin (1940). They gave an accurate photographic light curve and eclipse ephemeris with a rough estimate of the spectral type as A. Other than a few times of minimum and the $uvby$ indices (see below), the star was little studied until Lacy (1984) announced the discovery of double lines in high-resolution spectra. Lacy continued his spectroscopic program at Kitt Peak National Observatory (KPNO), assisted after 1998 by J. A. S., and also obtained absolute photometry in the UBV and $uvby\beta$ systems while he was a visitor at Mount Laguna Observatory in the autumn of 1989. Beginning in 1995, spectrometers operated by the Harvard-Smithsonian Center for Astrophysics (CfA) were used in an intensive campaign to obtain high-resolution spectra as well. In the middle of 2000 November, an automated photometric telescope at Kimpel Observatory on the campus of the University of Arkansas at Fayetteville began operation with WW Cam as one of its targets. By the end of 2001 April, it had obtained 5759 differential observations in the V filter with a standard error of 0.008 mag, more observations of an eclipsing binary than ever obtained before in less than one observing season. In this paper, we present the analysis of these photometric and spectroscopic data to determine accurate measurements of the absolute properties of this binary star system. The results are among the most accurate determinations to date for any eclipsing binary. We then compare our results to those of theory, where we find good agreement with models having an age of about 490 Myr.

2. TIMES OF MINIMUM AND THE ORBITAL PERIOD

Times of eclipse for WW Cam have been measured for nearly a century. All available estimates from the literature are collected in Table 1, along with six new measurements from the observations reported in this paper, the last six entries in Table 1 (the uncertainties of these timings are as follows: 8, 11, 10, 10, 8, and 30×10^{-5} days). There are 39 primary minima and 27 secondary minima, one of which gives a large residual and was excluded (it is listed in parentheses in the table). Uncertainties for the eclipse timings

[1] Some of the observations reported here were obtained with the Multiple Mirror Telescope, a joint facility of the Smithsonian Institution and the University of Arizona.

[2] Visiting Astronomer, Mount Laguna Observatory, San Diego State University, San Diego, CA.

[3] Visiting Astronomer, Kitt Peak National Observatory, National Optical Astronomy Observatory, which is operated by the Associated Universities for Research in Astronomy, Inc., under cooperative agreement with the National Science Foundation.

TABLE 1

Dates of Minima of WW Camelopardalis

HJD (2,400,000+)	Date	Type[a]	Method[b]	Cycle[c] (E)	$O-C$ (days)	Ref.
17,114.762	1905.7351	1	pg	−15315.0	−0.0367	1
27,100.384	1933.0743	2	pg	−10924.5	+0.0060	2
30,722.327	1942.9906	1	pg	−9332.0	+0.0132	2
30,764.374	1943.1057	2	pg	−9313.5	−0.0031	2
30,813.316	1943.2397	1	pg	−9292.0	+0.0276	2
30,973.587	1943.6785	2	pg	−9221.5	−0.0315	2
31,022.537	1943.8126	1	pg	−9200.0	+0.0072	2
36,460.543	1958.7010	1	pg	−6809.0	+0.0108	2
36,817.591	1959.6786	1	pg	−6652.0	−0.0163	2
37,222.473	1960.7871	1	pg	−6474.0	+0.0291	2
37,579.549	1961.7647	1	pg	−6317.0	+0.0301	2
37,669.377	1962.0106	2	pg	−6277.5	+0.0332	2
37,903.562	1962.6518	2	pg	−6174.5	−0.0412	2
37,911.596	1962.6738	1	pg	−6171.0	+0.0200	2
37,936.571	1962.7422	1	pg	−6160.0	−0.0230	2
37,944.569	1962.7640	2	pg	−6156.5	+0.0272	2
38,317.546	1963.7852	2	pg	−5992.5	+0.0087	2
38,473.382	1964.2119	1	pg	−5924.0	+0.0383	2
38,640.509	1964.6694	2	pg	−5850.5	+0.0121	2
38,739.462	1964.9403	1	pg	−5807.0	+0.0178	2
38,813.324	1965.1426	2	pg	−5774.5	−0.0245	2
39,403.549	1966.7585	1	v	−5515.0	−0.0092	3
39,592.347	1967.2754	1	pg	−5432.0	+0.0166	2
39,609.341	1967.3219	2	pg	−5424.5	−0.0347	2
39,940.352	1968.2282	1	pg	−5279.0	+0.0440	2
40,066.530	1968.5737	2	pg	−5223.5	+0.0073	2
40,073.359	1968.5924	2	v	−5220.5	+0.0132	3
40,149.553	1968.8010	1	pg	−5187.0	+0.0036	2
40,149.583	1968.8010	1	pg	−5187.0	+0.0336	2
40,288.2890	1969.1808	1	v	−5126.0	+0.0035	4
40,381.5310	1969.4361	1	v	−5085.0	−0.0034	4
40,422.4680	1969.5482	1	v	−5067.0	−0.0050	4
40,438.4020	1969.5918	1	v	−5060.0	+0.0085	4
40,514.552	1969.8003	2	pg	−5026.5	−0.0202	2
40,804.568	1970.5943	1	v	−4899.0	+0.0020	3
40,811.400	1970.6130	1	v	−4896.0	+0.0109	3
40,836.406	1970.6815	1	v	−4885.0	−0.0011	3
41,267.388	1971.8614	2	v	−4695.5	+0.0016	3
41,300.399	1971.9518	1	pg	−4681.0	+0.0218	2
41,383.370	1972.1790	2	pg	−4644.5	−0.0090	2
41,483.456	1972.4530	2	v	−4600.5	+0.0050	5
41,567.546	1972.6832	2	pg	−4563.5	−0.0564	2
41,567.573	1972.6833	2	pg	−4563.5	−0.0294	2
41,582.400	1972.7239	1	v	−4557.0	+0.0018	6
41,603.418	1972.7814	2	v	−4547.5	(−0.5742)	7
41,607.418	1972.7924	1	v	−4546.0	+0.0018	7
41,781.398	1973.2687	2	v	−4469.5	+0.0055	8
42,303.365	1974.6978	1	v	−4240.0	−0.0064	9
42,402.288	1974.9686	2	v	−4196.5	−0.0057	10
49,624.5462	1994.7421	1	pe	−1021.0	−0.0004	11
49,624.5465	1994.7421	1	pe	−1021.0	−0.0001	11
50,319.3520	1996.6444	2	pe	−715.5	−0.0001	12
50,667.3343	1997.5971	2	pe	−562.5	+0.0047	12
50,675.3063	1997.6189	1	pe	−559.0	+0.0039	12
50,843.6054	1998.0797	1	pe	−485.0	+0.0002	12
50,852.7028	1998.1046	1	pe	−481.0	+0.0001	12
50,868.6209	1998.1482	1	pe	−474.0	−0.0023	12
51,134.7232	1998.8767	1	pe	−357.0	−0.0005	13
51,474.7295	1999.8076	2	pe	−207.5	+0.0009	14
51,607.7921	2000.1719	1	pe	−149.0	+0.0008	15
51,865.91908	2000.8786	2	pe	−35.5	+0.0000	16
51,912.55566	2001.0063	1	pe	−15.0	−0.0003	16
51,913.68052	2001.0094	2	pe	−14.5	−0.0002	16
51,914.83041	2001.0125	1	pe	−14.0	+0.0001	16
51,946.67150	2001.0997	1	pe	0.0	+0.0001	16
51,979.63790	2001.1900	2	pe	14.5	+0.0007	16

[a] (1) Primary eclipse; (2) secondary eclipse.

[b] (pg) Photographic; (v) visual; (pe) photoelectric or CCD.

[c] Integral cycle numbers denote primary minima, half-integral cycle numbers denote secondary minima.

References.—(1) Huruhata & Gaposchkin 1940; (2) von Zschocke 1973; (3) Braune 1972; (4) Kundera 2001 (http://www.oa.uj.edu.pl/ktt/); (5) Peter 1972a; (6) Diethelm 1972; (7) Peter 1972b; (8) Braune, Hübscher, & Mundry 1977; (9) Diethelm 1974; (10) Diethelm 1975; (11) Agerer & Hübscher 1995; (12) Lacy et al. 1998; (13) Lacy, Marcrum, & İbanoğlu 1999; (14) Lacy, Hood, & Straughn 2001; (15) Nelson 2001; (16) this paper.

were adopted as published and used to determine weights or were determined iteratively for the photographic, visual, and photoelectric measurements that did not list uncertainties (0.026, 0.0078, and 0.0040 days, respectively). A weighted least-squares solution gives the following linear ephemeris:

$$\text{Min I} = \text{HJD } 2,451,946.671403(71) + 2.27436322(16)E ,$$
$$\text{Min II} = \text{HJD } 2,451,947.796123(83) + 2.27436322(16)E ,$$

with a phase difference between the primary and secondary eclipse of 0.494521 ± 0.000073. This indicates that the eccentricity of the orbit is small, but clearly significant. Separate fits to the primary and secondary minima give nearly identical periods (no detectable apsidal motion): $P_{\rm I} = 2.27436323 \pm 0.00000018$ days and $P_{\rm II} = 2.27436317 \pm 0.00000038$ days. The ephemeris above was adopted for use in our spectroscopic and light-curve solutions below.

3. SPECTROSCOPIC OBSERVATIONS AND REDUCTIONS

WW Cam was observed spectroscopically at KPNO beginning in 1983 December. A variety of gratings and detectors were used with the 2.1 m reflector or coudé feed telescope and the coudé spectrometer between then and the last observation in 2001 January. The resolution (2 pixels) was typically 0.025 nm, with coverage between 10 and 32 nm centered near a wavelength of 450 nm. The signal-to-noise ratio (S/N) was typically 50–100. Wavelength calibration errors contributed less than 0.5 km s^{-1} to the radial velocity uncertainties, shown later to be about 2.4 km s^{-1}. A total of 44 spectrograms yielded usable radial velocities.

Projected rotational velocities ($v \sin i$) were determined by comparing line widths of the binary components' unblended features with artificially broadened features in the spectra of comparison stars with known small values of $v \sin i$. These comparison stars were chosen to be of nearly the same spectral type as WW Cam and were observed with the same instrumental configuration as the binary. The reference stars used were 68 Tau (=HR 1389, A2 IV–V, $v \sin i = 18$ km s^{-1}; Hoffleit & Jaschek 1982) and HR 8404 (=21 Peg, B9.5 V, $v \sin i = 4$ km s^{-1}; Fekel 1999). From these comparisons in 40 of the best spectrograms, we find $v \sin i$ values of 42.8 ± 0.5 and 41.9 ± 0.9 km s^{-1} for the primary and secondary components of WW Cam, respectively. The primary star is the hotter one, the one in back during primary eclipse; for WW Cam, this turns out to be the larger, more massive star. Later, these directly measured $v \sin i$ values will be shown to be not significantly different from the theoretical synchronous values.

Line strengths (equivalent widths) of the four strongest metal lines in the 450 nm region were estimated on 40 of the best KPNO spectrograms of WW Cam. These equivalent widths were converted into the approximate values each of the binary star components would have as single stars by using the luminosity ratio (V band) found from the photometric analysis below. The binary star line strengths were compared with those in spectrograms of bright main-sequence stars with well-known spectral types between B7 and F2. The same equipment and settings were used for the comparison stars as for the binary star. The intrinsic strengths of lines of the primary and secondary in WW Cam are as follows: 4481 Å Mg II, Fe I line, primary equivalent width 0.536 Å, secondary equivalent width 0.596 Å; 4501 Å Ti II line, 0.237 Å, 0.242 Å; 4508 Å Fe II line, 0.206 Å, 0.233 Å; 4550 Å Fe II, Ti II line, 0.424 Å, 0.448 Å. These line strengths are stronger than any of the 14 comparison stars used, including HR 7562, classified as A1m (see Table 2). We therefore conclude that both components of WW Cam are chemically peculiar, probably Am stars. The fact that the secondary's line strengths are slightly stronger than those of the primary component may indicate that the secondary's atmosphere is richer in heavy elements than that of the primary.

The mean line strength ratio of the primary and secondary lines in the four strongest metal lines 4481 Å Mg II, Fe I, 4501 Å Ti II, 4508 Å Fe II, and 4550 Å Fe II, Ti II was 1.13 ± 0.05 in the 26 spectrograms with the highest S/N. This line strength ratio should be very close to the photometric solution's luminosity ratio, but perhaps not quite exactly the same since the two components differ slightly in temperature, and we are comparing an equivalent width ratio in the blue to a light ratio in the yellow. In fact, the

TABLE 2
Spectral Line Strengths in Main-Sequence Stars

HR	Spectral Type	EW (Å) 4481 Å Mg II, Fe I	4501 Å Ti II	4508 Å Fe II	4550 Å Fe II, Ti II
811	B7 V	0.303	0.012	0.044	0.093
2010	B9 IV	0.379	0.046	0.076	0.157
8404	B9.5 V	0.363	0.046	0.061	0.159
7001	A0 V	0.283	0.060	0.057	0.159
4300	A1m	0.456	0.137	0.150	...
7562	A1m	0.480	0.171	0.179	0.418
8641	A1 IV	0.423	0.105	0.105	0.293
1389	A2 IV	0.550	0.149	0.144	0.368
4359	A2 V	0.430	0.117	0.113	0.302
2238	A2 V	0.444	0.126	0.102	0.281
6548	A2 V	0.432	0.093	0.096	...
8155	A5 IV	0.385	0.221	0.176	...
4825/6	F0 V	0.374	0.179	0.114	0.340
5447	F2 V	0.257	0.136	0.102	0.286

light-curve solution (below) gives a ratio of 1.18 ± 0.04, not significantly different from the directly measured line ratio. This close agreement is an important cross-check on the accuracy of the photometric orbit.

Radial velocities of the components were measured by cross-correlation with the FXCOR task in IRAF,[4] using standard stars (same as above) with known radial velocities (taken from Fekel 1999) as templates. Our measurements from KPNO spectrograms with apparently unblended lines were then fitted with a spectroscopic orbit that had reasonably small residual standard errors (about 2.4 km s^{-1}). The resultant radial velocity semiamplitudes, however, did not agree within the error estimates with those of the CfA radial velocity program described below. An intensive scrutiny of both methods followed. As part of this analysis, individual line wavelengths of the six most favorable absorption lines in the 4500 Å region of the KPNO spectrograms were measured and radial velocities determined by using the rest wavelengths of the lines as measured in 12 spectrograms of the standard star 68 Tau. The results indicated a bias of about 1.3 km s^{-1} in measured radial velocities of the 4481 Å Mg II, Fe I line when it was blueshifted and a bias of about 1.4 km s^{-1} in measured radial velocities of the 4550 Å Fe II, Ti II line when redshifted. These biases presumably originate from unrecognized blending with relatively weak stellar features of the oppositely directed component or blending with an interstellar feature. Since these are the two strongest lines in this spectral region, their biases had a very significant effect on the cross-correlation radial velocities. By omitting radial velocity measurements of these biased features, spectroscopic orbits based on KPNO spectrograms yielded parameters in reasonably good accord with the CfA measurements. In addition, residuals from the mean velocities based on individual line measurements were essentially the same as those of the cross-correlation method (2.4 km s^{-1}). Adopted KPNO velocities and residuals from the final spectroscopic orbit are listed in Table 3.

Our observations of WW Cam at the CfA were collected mostly with the echelle spectrograph on the 1.5 m Tillinghast reflector at the F. L. Whipple Observatory on Mount Hopkins (Arizona), where the binary star was monitored from 1995 April to 1998 October. Occasionally, we observed with an identical spectrograph on the Multiple Mirror Telescope (also atop Mount Hopkins). A total of 41 spectrograms were recorded with a photon-counting Reticon detector covering a single echelle order centered at 518.7 nm. The resolution is 0.015 nm ($\lambda/\Delta\lambda \sim 35{,}000$), and the spectra span about 4.5 nm. The S/N values range from about 15 to 40 per resolution element. The zero point of the velocity system was monitored by means of nightly exposures of the dusk and dawn sky in the manner described by Latham (1992). The accuracy of the CfA velocity system, which is within about 0.1 km s^{-1} of the reference frame defined by minor planets in the solar system, is documented in the previous citation and also by Stefanik, Latham, & Torres (1999).

Radial velocities were determined in essentially the same way as those described by Torres et al. (2000) by using the CfA implementation of TODCOR (Zucker & Mazeh 1994), a two-dimensional cross-correlation algorithm that uses two templates, one for each component of the binary star.

[4] IRAF is distributed by the National Optical Astronomy Observatory.

TABLE 3

KPNO Radial Velocities of WW Camelopardalis and Residuals from the Final Spectroscopic Orbit

HJD (2,400,000+)	RV_A (km s^{-1})	RV_B (km s^{-1})	$(O-C)_A$ (km s^{-1})	$(O-C)_B$ (km s^{-1})	Orbital Phase
45,683.7202.....	−120.0	124.0	0.77	−1.97	0.284
45,684.7875.....	121.5	−128.5	−3.36	−2.66	0.753
45,685.7688.....	−116.0	117.9	−1.06	−2.08	0.184
46,071.7968.....	68.0	−59.8	3.46	4.21	0.915
46,156.6198.....	−117.1	128.6	4.01	2.29	0.210
47,781.9414.....	106.7	−106.0	−0.40	1.63	0.837
48,146.9135.....	−119.4	119.3	−4.97	−0.17	0.309
48,147.9901.....	119.7	−128.3	−2.66	−5.02	0.782
51,243.6714.....	71.5	−70.2	−0.98	1.94	0.902
51,244.6488.....	−106.4	114.7	−0.28	3.76	0.332
51,246.6359.....	−121.4	124.9	−1.03	−0.65	0.206
51,246.6788.....	−122.4	130.5	0.86	1.99	0.225
51,247.6731.....	108.3	−105.6	1.48	1.75	0.662
51,449.9613.....	76.7	−77.4	−1.23	0.33	0.605
51,450.0051.....	90.0	−87.8	1.07	1.21	0.624
51,451.8077.....	−57.6	62.8	1.15	0.42	0.417
51,451.8507.....	−47.0	48.4	−1.59	−0.31	0.435
51,452.8337.....	91.2	−95.5	−1.61	−2.51	0.868
51,452.8843.....	77.5	−79.0	−2.77	1.13	0.890
51,453.8319.....	−116.5	118.9	−1.30	−1.35	0.307
51,453.8747.....	−107.8	113.3	1.02	−0.41	0.325
51,453.9129.....	−102.5	106.8	−0.67	0.26	0.342
51,455.8892.....	−122.5	127.2	−1.15	0.65	0.211
51,455.9939.....	−121.5	129.4	2.54	0.08	0.257
51,548.8618.....	−66.7	73.3	0.60	2.15	0.090
51,548.9091.....	−79.8	85.1	0.80	0.32	0.110
51,548.9597.....	−93.8	100.0	−0.55	2.25	0.133
51,549.5808.....	−63.8	71.4	2.21	1.58	0.406
51,550.6220.....	95.8	−96.7	0.87	−1.54	0.864
51,550.6722.....	82.2	−81.6	−0.61	1.13	0.886
51,551.6450.....	−115.0	116.9	−1.93	−1.17	0.313
51,552.8092.....	109.2	−110.5	−2.28	1.63	0.825
51,553.8551.....	−121.1	126.2	−0.61	0.52	0.285
51,553.8981.....	−113.6	123.6	2.34	2.59	0.304
51,553.9413.....	−106.7	114.7	3.00	0.08	0.323
51,789.9874.....	−79.6	81.5	−0.13	−2.13	0.109
51,792.8985.....	−76.3	80.5	0.68	−0.57	0.389
51,794.8761.....	−121.6	127.1	2.39	−2.16	0.258
51,795.8620.....	116.6	−115.9	−0.19	1.67	0.692
51,795.9745.....	123.3	−120.4	−1.38	5.26	0.741
51,906.6896.....	−57.3	58.2	−1.36	−1.30	0.421
51,907.6981.....	94.9	−95.8	0.21	−0.89	0.864
51,909.7717.....	119.3	−125.4	−3.99	−1.16	0.776
51,910.6864.....	−117.4	117.6	−4.52	−0.28	0.178

The templates were selected from a large library of synthetic spectra based on the latest model atmospheres by R. Kurucz, computed specifically for the wavelength of our observations. These synthetic spectra have been calculated over a wide range of effective temperatures, projected rotational velocities, metallicities, and surface gravities. Initially, we used templates with temperatures of 8750 and 8500 K and log g values of 4.0. The temperature difference between the components was strongly constrained by the observed surface brightness of the secondary component, which was found from analysis of the differential photometry (discussed below). The optimum rotational velocities for this combination were 46 and 45 km s^{-1}, slightly higher than the KPNO results.

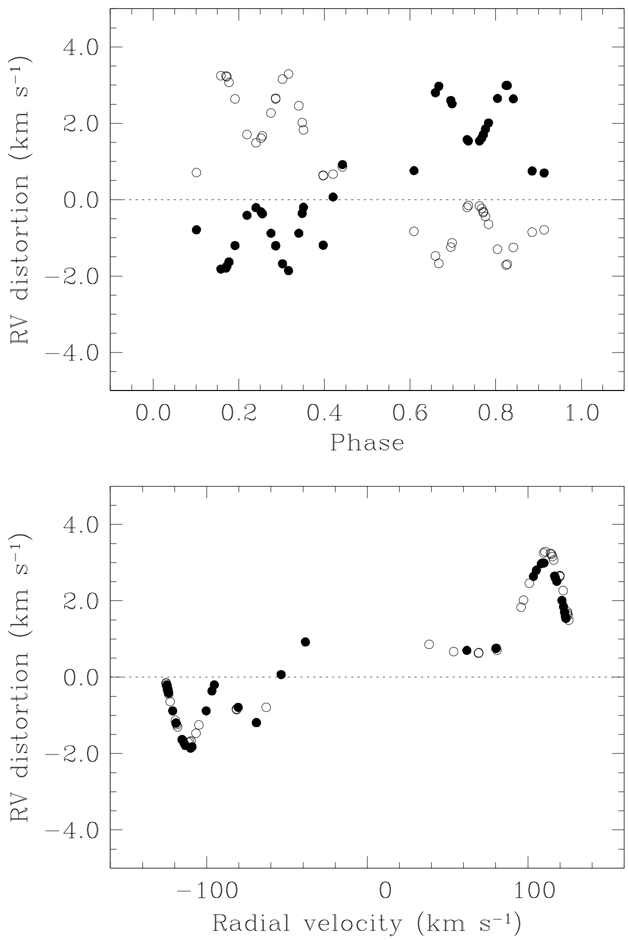

FIG. 1.—Systematic distortions in the raw TODCOR velocities for WW Cam, as determined from simulations with synthetic binary spectra (see text) and plotted as a function of orbital phase and radial velocity. These differences have been applied as corrections to the raw CfA velocities. Filled circles are for the primary, and open circles are for the secondary.

TABLE 4

CfA RADIAL VELOCITIES OF WW CAMELOPARDALIS AND RESIDUALS FROM THE FINAL SPECTROSCOPIC ORBIT

HJD (2,400,000+)	RV_A (km s^{-1})	RV_B (km s^{-1})	$(O-C)_A$ (km s^{-1})	$(O-C)_B$ (km s^{-1})	Orbital Phase
49,965.0077.....	119.52	−120.20	1.93	−1.51	0.695
50,003.9195.....	117.96	−120.12	0.17	−1.22	0.804
50,030.8830.....	103.67	−108.97	−1.98	−2.52	0.659
50,059.8535.....	−68.05	73.52	3.64	−1.82	0.397
50,061.8514.....	−122.74	127.42	−0.47	0.23	0.276
50,088.7482.....	−75.11	79.96	0.27	0.84	0.102
50,092.8676.....	69.61	−64.34	4.20	0.86	0.913
50,141.7300.....	−74.61	80.45	−2.76	4.95	0.397
50,148.6064.....	−53.26	59.22	2.96	−0.26	0.420
50,408.8406.....	107.44	−109.22	2.23	−3.22	0.841
50,409.8525.....	−122.81	119.27	−2.35	−6.07	0.286
50,441.7632.....	−117.00	113.62	−4.87	−3.17	0.317
50,448.6576.....	−101.20	103.55	−1.91	−0.08	0.348
50,473.8893.....	−44.04	42.41	−3.21	−1.29	0.442
50,474.6394.....	123.96	−121.17	0.36	3.68	0.772
50,476.6760.....	109.08	−111.81	0.36	−2.20	0.667
50,499.6353.....	122.83	−129.82	−1.55	−4.16	0.762
50,564.6327.....	−103.21	110.40	−0.41	3.17	0.340
50,652.9465.....	−110.23	116.94	0.18	1.91	0.171
50,653.9443.....	81.26	−81.09	0.84	−0.49	0.609
50,740.8605.....	117.23	−113.20	5.74	−0.76	0.825
50,741.9474.....	−117.26	122.58	−0.79	1.34	0.303
50,743.0037.....	128.51	−128.19	4.48	−2.89	0.767
50,743.9680.....	−116.58	113.29	0.45	−8.53	0.191
50,768.9437.....	−111.81	119.42	−0.66	3.62	0.173
50,773.7504.....	−119.61	127.32	0.87	1.96	0.286
50,792.8840.....	122.81	−124.56	4.34	−4.96	0.699
50,793.9303.....	−104.38	109.89	1.39	−0.39	0.159
50,797.8573.....	82.37	−87.54	−0.46	−4.48	0.885
50,798.6917.....	−127.12	127.60	−2.70	−1.79	0.252
50,798.6995.....	−122.20	124.93	2.07	−4.32	0.256
50,799.7867.....	119.13	−122.83	−4.95	2.52	0.734
50,799.7932.....	122.65	−126.38	−1.64	−0.82	0.737
50,821.6601.....	−96.97	102.58	0.86	0.45	0.351
50,822.6154.....	126.25	−124.22	2.58	0.71	0.771
50,822.6283.....	124.08	−120.48	1.06	3.78	0.777
50,822.6431.....	120.47	−117.00	−1.62	6.31	0.783
50,823.6343.....	−121.75	128.67	0.98	1.01	0.219
50,825.8128.....	−113.03	121.32	−0.34	3.95	0.177
50,829.5668.....	112.56	−112.73	2.03	−1.27	0.828
50,914.6565.....	−124.87	128.24	−0.43	−1.18	0.240

A more detailed analysis was then done, in which the values of log g were fixed at values indicated by initial analysis of the KPNO radial velocities and the differential photometry, log $g = 4.1$ and 4.2. Rotational velocities were fixed at 46 and 45 km s^{-1}, and a grid of analyses of the CfA spectrograms were run in which a variety of values for temperature and metallicity were assumed. The optimum model fitting the data was one with effective temperatures of 8900 and 8760 K and a metallicity [m/H] $= +0.3$. The higher-than-solar metal abundance is consistent with the metallic-lined nature of the system described earlier.

As in previous studies using similar spectroscopic material, systematic errors in the CfA radial velocities were evaluated by performing numerical simulations as described in more detail by Torres et al. (2000). Distortions in the raw velocities showing a clear pattern with phase (or velocity) were found to be significant (up to 4 km s^{-1}), confirming the importance of systematic effects for this particular system (see Fig. 1). The final CfA radial velocities, after correction for these effects, are listed in Table 4.

Orbital parameters resulting from analyses of all the radial velocities, separately for both KPNO and CfA and also combined, are listed in Table 5. For the combined solution, we allowed for a possible zero-point difference between the two velocity sets, which turned out to be insignificant, and weighted the observations of the primary and secondary separately for each group. The ephemeris adopted is that of § 2. The observations and fitted model from the combined solution are shown in Figure 2. The agreement between all KPNO and CfA parameters analyzed separately is good except for that of the primary component's semiamplitude, K_A, where the two estimates differ by about 2.8 σ. This difference may be due to some unrecognized systematic errors in our methods of analysis. Because of this significant difference, we decided to double the error estimate for this parameter in the adopted joint solution (the doubled value is listed in the last column of Table 5). The increase in this error estimate also propagates through to the error estimates of masses, mass ratio, semimajor axis, etc.

TABLE 5

SPECTROSCOPIC ORBITAL PARAMETERS OF WW CAMELOPARDALIS

Element	EPNO	CfA	Combined
Fixed quantities:			
P (days)	2.27436322	2.27436322	2.27436322
Min I (HJD − 2,400,000)	51,946.671403	51,946.671403	51,946.671403
Adjusted quantities:			
γ (km s^{-1})	+1.00 ± 0.22	+0.92 ± 0.31	+0.91 ± 0.30
ΔRV (km s^{-1}) (CfA − KPNO)	...	...	−0.15 ± 0.38
K_A (km s^{-1})	124.12 ± 0.38	125.24 ± 0.43	124.62 ± 0.58
K_B (km s^{-1})	127.76 ± 0.38	127.78 ± 0.58	127.76 ± 0.31
e	0.0098 ± 0.0017	0.0099 ± 0.0035	0.0094 ± 0.0015
ω_A (deg)	141 ± 12	120 ± 20	134 ± 10
Derived quantities:			
T (HJD − 2,400,000)	51,947.022 ± 0.078	51,946.87 ± 0.13	51,946.949 ± 0.076
$a_A \sin i$ (10^9 m)	3.882 ± 0.012	3.917 ± 0.014	3.897 ± 0.019
$a_B \sin i$ (10^9 m)	3.995 ± 0.012	3.996 ± 0.019	3.995 ± 0.010
$a \sin i$ ($R_\odot$)	11.318 ± 0.025	11.369 ± 0.034	11.340 ± 0.030
$M_A \sin^3 i$ ($M_\odot$)	1.910 ± 0.013	1.928 ± 0.020	1.917 ± 0.013
$M_B \sin^3 i$ ($M_\odot$)	1.855 ± 0.013	1.889 ± 0.016	1.870 ± 0.018
$q = M_B/M_A$	0.9715 ± 0.0043	0.9801 ± 0.0058	0.9755 ± 0.0053
Other quantities pertaining to the fit:			
$N_{\rm obs}$	44	41	44/41
Time span (yr)	17.0	2.6	17.0
σ_A (KPNO) (km s^{-1})	2.02	...	2.08
σ_B (KPNO) (km s^{-1})	2.07	...	2.03
σ_A (CfA) (km s^{-1})	...	2.38	2.46
σ_B (CfA) (km s^{-1})	...	3.24	3.17

4. PHOTOMETRIC OBSERVATIONS AND LIGHT-CURVE SOLUTION

Absolute photometry on both the *UBV* and *uvby*β photometric systems was obtained by Lacy. Results of the *UBV* program are given by Lacy (1992). The components of WW Cam are early A-type stars in a region of the *UBV* color-color diagram where the reddening vector is nearly parallel with the main sequence, making it difficult to estimate the reddening and intrinsic color of the stars. Observations in the *uvby*β system are better suited for this kind of determination. The *uvby*β observations were obtained while visiting Mount Laguna Observatory in the autumn of 1989. Details of the observing program are reported elsewhere (Lacy 2002).

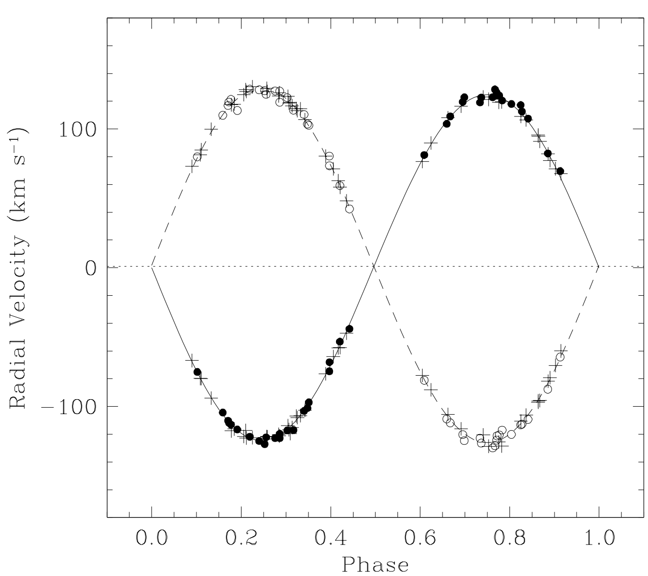

FIG. 2.—Spectroscopic observations and adopted orbit for WW Cam. The filled circles are for the CfA observations of the primary, the open circles are for the CfA observations of the secondary, and the plus signs are the velocity measurements from KPNO.

Four observations of WW Cam on the standard system were made on separate nights. Mean values and standard errors of the means outside eclipse are as follows: $V = 10.157 \pm 0.006$, $b-y = 0.358 \pm 0.003$, $m_1 = 0.158 \pm 0.005$, $c_1 = 1.032 \pm 0.009$, and $\beta = 2.888 \pm 0.005$. The values of the standard errors are consistent with those of standard stars observed on the same nights. The value of V is consistent with that of Lacy (1992). The values of $b-y$, m_1, and c_1 are consistent with those of Hilditch & Hill (1975) but are more accurate. Applying the prescription of Crawford (1979), we find that the intrinsic color index is $(b-y)_0 = 0.064 \pm 0.010$, and $E_{b-y} = 0.294 \pm 0.010$, which corresponds to $E_{B-V} = 0.397 \pm 0.014$ and $(B-V)_0 = 0.113 \pm 0.014$. We have doubled the standard errors in all of these photometric estimates to try to account for the systematic errors inherent in corrections for chemically peculiar stars. According to Popper's (1980) Table 1, these color indices correspond to a mean spectral type A4 star with an effective temperature of 8300 ± 135 K. As a result of the analysis of the differential photometry in V below, we know that the secondary surface brightness value strongly constrains the difference in surface brightness parameters of the two components to be $\Delta F_V = 0.005$, which, through Table 1 of Popper (1980), leads to $\Delta \log T = 0.006$, and $\log T_p = 3.922 \pm 0.007$ ($T_p = 8350 \pm 135$ K) and $\log T_s = 3.916 \pm 0.007$ ($T_s = 8240 \pm 135$ K). We adopt spectral types of A4m + A4m.

The $uvby\beta$ indices can be used to estimate the metallicity of stellar atmospheres with the calibration of Strömgren (1966), $[Fe/H] = 0.3 - 12\delta_{m_1}$, which gives for WW Cam $[Fe/H] = 0.96$, about 10 times solar metallicity in the surface layers, at least. This is independent confirmation of the conclusion given above that these stars are definitely metallic-lined Am types.

Kimpel Observatory consists of a Meade 10 inch (0.25 m) f/6.3 LX-200 telescope with a Santa Barbara Instruments Group ST8 CCD camera (binned 2×2 to produce 765×510 pixel images with $2''.3$ square pixels) inside a Technical Innovations Robo-Dome and is controlled automatically by an Apple Macintosh G4 computer. The observatory is located on top of Kimpel Hall on the Fayetteville campus, with the control room directly beneath the observatory inside the building. Sixty second exposures through a Bessel *V* filter (2.0 mm of GG 495 and 3.0 mm of BG 39) were read out and downloaded to the control computer over a 30 s interval, then the next exposure was begun. The observing cadence was therefore about 90 s per observation. The variable star would frequently be monitored continuously for 4–8 hr. WW Cam was observed on 54 nights during part of one observing season from 2000 November 14 to 2001 April 30.

The images were analyzed by a virtual measuring engine application written by C. H. S. L. that automatically located the variable, comparison, and check stars in the image, measured their brightnesses, subtracted the corresponding sky brightness, and corrected for the differences in air mass between the stars. Extinction coefficients were determined nightly from the comparison star measurements. They averaged 0.25 mag per air mass. The comparison star was GSC 04073-0510 (10.1 mag), and the check star was GSC 04073-1078 (9.3 mag). Both comparison stars are within $4'$ of the variable star. The comparison-minus-check magnitude differences were constant at the level of 0.008 mag for the standard deviation of the magnitude differences and 0.008 mag for the standard deviation of the nightly means. The resulting 5759 *V*-magnitude differences (variable minus comparison) are listed in Table 6 and shown in Figure 3.

The light-curve fitting was done with the Nelson-Davis-Etzel (NDE) model as implemented in the code EBOP (Etzel 1981; Popper & Etzel 1981), and the ephemeris adopted is that of § 2. The main adjustable parameters are the relative surface brightness of the secondary star (J_s) in units of that of the primary, the relative radius of the primary (r_A) in units of the separation, the ratio of radii ($k = r_B/r_A$), the inclination of the orbit (i), and the geometric factors $e \cos \omega$ and $e \sin \omega$, which account for the orbital eccentricity. Auxiliary parameters needed in the analysis include the gravity-brightening coefficient, which we adopt as 0.95 for both components based on their temperatures (Claret 1998). Limb-darkening coefficients (u) were included as variables to be fitted. The difference between the limb-darkening coefficients was fixed at the theoretical value (Claret 1998) based on the temperature difference derived from the J_s value. The mass ratio ($q = M_B/M_A = 0.9755$) was adopted from the spectroscopic analysis in § 3. Other adjusted parameters were the magnitude at quadrature and the phase of primary eclipse. The fitting procedure converged to the solution listed in Table 7 and shown in Figures 3–5. There is good agreement between the fitted values of $e \cos \omega$ and $e \sin \omega$ and those in the spectroscopic analysis above. A test for third light was not significantly different from zero (0.003 ± 0.003).

According to the fitted orbit, the fraction of light lost from the primary component during primary eclipse is 86.3%; the corresponding fraction during secondary eclipse is 94.5%. Both eclipses are deep and nearly complete. Popper (1984a) found that accurate information about the limb-darkening coefficients in similar cases requires data sets containing a couple of hundred observations at our precision within minima. Our data set contains a couple of

TABLE 6

Differential Magnitudes for WW Camelopardalis in *V*

Orbital Phase	ΔV	HJD − 2,400,000
0.02097	0.155	51,862.56766
0.02148	0.160	51,862.56882
0.02200	0.144	51,862.57000
0.02251	0.133	51,862.57116
0.02302	0.133	51,862.57232
0.02354	0.110	51,862.57350
0.02405	0.102	51,862.57466
0.02457	0.107	51,862.57584
0.02509	0.086	51,862.57702
0.02560	0.085	51,862.57818
0.02612	0.053	51,862.57936
0.02663	0.068	51,862.58052
0.02714	0.052	51,862.58169
0.02765	0.040	51,862.58284
0.02816	0.045	51,862.58401
0.02867	0.045	51,862.58517
0.02918	0.034	51,862.58633
0.02970	0.018	51,862.58750
0.03020	0.007	51,862.58865
0.03072	0.011	51,862.58982
0.03122	−0.005	51,862.59097
0.03174	−0.012	51,862.59214
0.03225	−0.012	51,862.59330
0.03275	−0.029	51,862.59445

Note.—Table 6 is presented in its entirety in the electronic edition of the Astronomical Journal. A portion is shown here for guidance regarding its form and content.

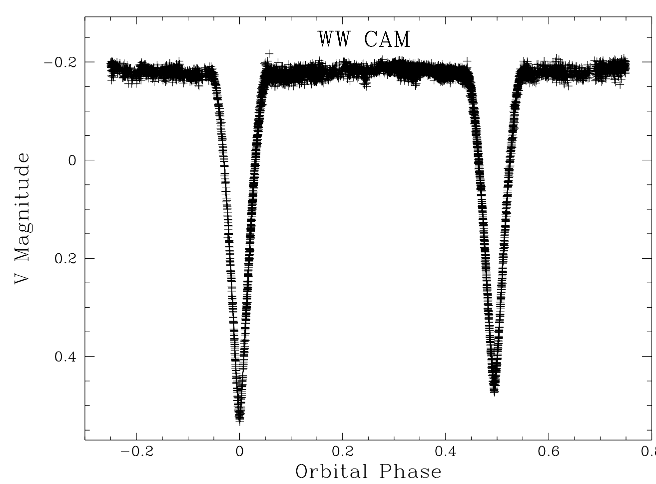

Fig. 3.—Differential magnitudes in *V* and the fitted photometric orbit for WW Cam. The fitted orbit is the solid curve through the observed points.

TABLE 7
FITTED PHOTOMETRIC ORBIT FOR WW CAMELOPARDALIS

Parameter	Symbol	Fitted Value
Surface brightness of secondary star	J_s	0.950 ± 0.003
Radius of primary (hotter) star	r_p	0.1684 ± 0.0013
Ratio of radii	k	0.946 ± 0.015
Orbital inclination (deg)	i	88.29 ± 0.06
	$e \cos \omega$	-0.00876 ± 0.00006
Eccentricity factor	$e \sin \omega$	$+0.0047 \pm 0.0014$
	u_p	0.494 ± 0.017
Limb-darkening coefficient	u_s	0.499 ± 0.017
Normalized luminosity of primary star	L_p	0.541 ± 0.009
Standard error (mag)	σ	0.008189
Number of observations	N	5759

thousand observations in eclipse, so it is reasonable to expect the limb-darkening coefficients to be well determined by the fit, as is indicated by the formal errors of the fit. The fitted mean value of 0.496 ± 0.017 may be compared with theoretical values for solar composition by Al-Naimiy (1978) of 0.51, Wade & Rucinski (1985) of 0.477, and Díaz-Cordovés, Claret, & Giménez (1995) of 0.591. Since the surface chemical composition of these two stars is quite metal-rich, such comparisons are problematic.

5. ABSOLUTE DIMENSIONS

The combination of the spectroscopic results of Table 5 with the light-curve results in Table 7 leads to the absolute dimensions and masses for WW Cam shown in Table 8. Table 1 of Popper (1980) has been used for the radiative quantities. He adopted the bolometric corrections of Hayes (1978). The masses are determined to an accuracy of 0.7% and 1.0%, and the radii are both good to about 0.8%. The corresponding theoretical rotational velocities ($v \sin i$ values) corresponding to the mean orbital motion (circular orbit) and to the motion at perihelion (eccentric orbit) differ by little because the eccentricity is so small. Either set of values is consistent with the KPNO observed values; the CfA observed values are slightly larger, but not significantly larger than these.

6. DISCUSSION

With the mass and radius of each component of WW Cam determined to better than 1% and the effective temperatures to better than 2%, we proceed in this section to compare the observations with evolutionary models computed specifically for this system, as well as with the predictions from tidal theory.

The evolutionary code we used is that by Claret (1995). Further details of the input physics are described by Claret & Giménez (1992). Convection in these models is treated with the standard mixing-length prescription, with a fixed mixing-length parameter of $1.52H_p$ that gives the best fit between a solar model and the observed properties of the Sun. A moderate amount of core overshooting is assumed ($\alpha_{\rm ov} = 0.20H_p$), although in the case of WW Cam this effect is insignificant due to the unevolved nature of the system (see below).

In Figure 6, we show evolutionary tracks computed for the exact mass of each component for a heavy-element abundance of $Z = 0.020$ and a helium abundance of $Y = 0.282$, which provides an excellent fit to the observations. The implied enrichment law, $dY/dZ = 2.1$, is in line with recent determinations (see, e.g., Peimbert 1993; Pagel & Portinari 1998; Izotov & Thuan 1998). Additional tracks for the primary corresponding to slightly different metal abundances ($dZ = \pm\ 0.001$) and the same enrichment law are shown for comparison (*dotted lines*), along with three

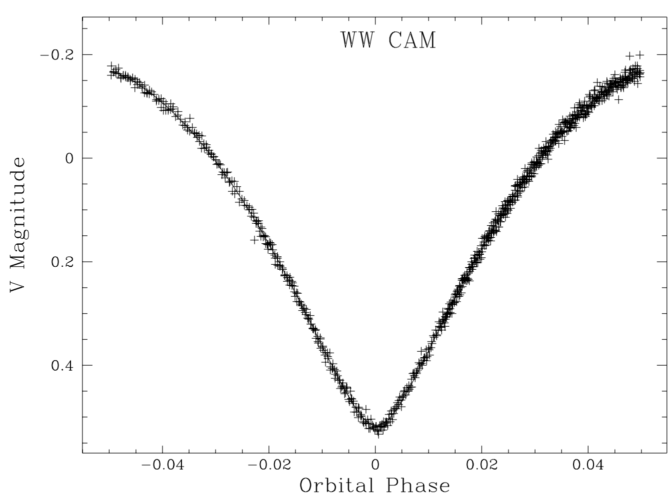

FIG. 4.—Primary eclipse of WW Cam

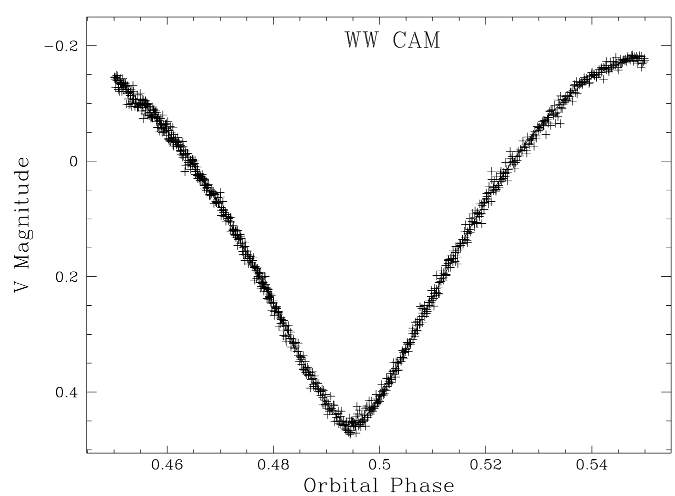

FIG. 5.—Secondary eclipse of WW Cam

TABLE 8
Absolute Properties of WW Camelopardalis

Parameter	Primary	Secondary
Mass ($M_\odot$)	1.920 ± 0.013	1.873 ± 0.018
Radius ($R_\odot$i)	1.911 ± 0.016	1.808 ± 0.014
log g (cm s^{-2})	4.1586 ± 0.0077	4.1960 ± 0.0086
Mean density (g cm^{-3})	0.3877 ± 0.0099	0.447 ± 0.012
v sin i (km s^{-1}):		
KPNO	42.8 ± 0.5	41.9 ± 0.9
CfA	46 ± 3	45 ± 3
v_{sync} (km s^{-1}):		
Circular	42.5 ± 0.3	40.2 ± 0.3
Eccentric	43.4 ± 0.4	41.0 ± 0.4
Semimajor axis ($R_\odot$)	11.345 ± 0.030	
log T_{eff}	3.922 ± 0.007	3.916 ± 0.007
log L (solar units)	1.20 ± 0.03	1.13 ± 0.03
M_{bol}(mag)	1.63 ± 0.06	1.81 ± 0.06
M_V (mag)	1.67 ± 0.06	1.84 ± 0.06
F_V	3.918 ± 0.006	3.913 ± 0.006
$m - M$ (mag)	7.88 ± 0.07	
Distance (pc)	376 ± 12	

isochrones. The difference in the effective temperatures that we measure for the components, which is derived essentially from the light curves, is well matched by the separation between the tracks, which depends on the mass ratio. The system is seen to lie quite near the zero-age main sequence. The ages we infer from the measured radii of the two components are log $t = 8.716$ and log $t = 8.642$ for the primary and secondary, respectively, while the values we derive

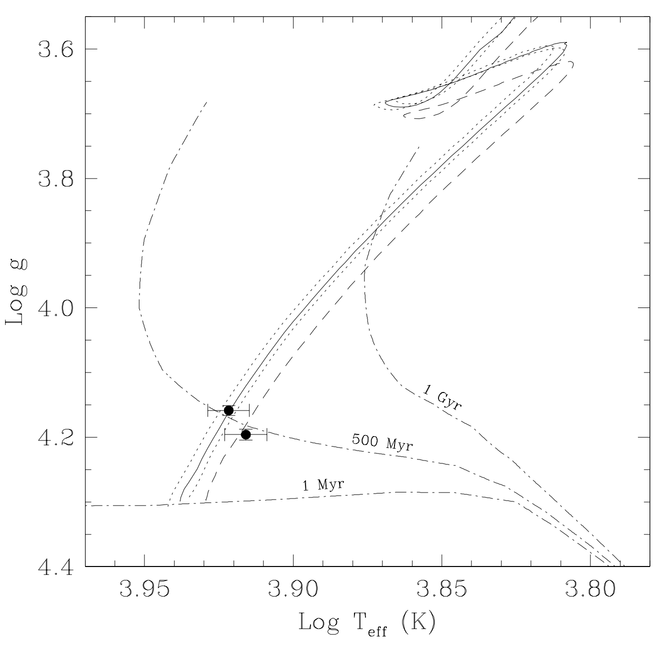

Fig. 6.—Evolutionary tracks for the primary (*solid curve*) and secondary (*dashed curve*) of WW Cam from the models by Claret (1995) for a chemical composition represented by $Z = 0.020$ and $Y = 0.282$. The observed values of log g and log T_{eff} are indicated, with error bars. The uncertainty in the position of each track due to the errors in the mass is approximately of the same size as the points. Additional tracks for the primary (*dotted lines*) for $Z = 0.019$ (*left*) and $Z = 0.021$ (*right*) illustrate the sensitivity to the heavy-element abundance for the same enrichment law. Three isochrones (*dot-dashed lines*) are shown for reference: 1 Myr (representative of the zero-age main sequence), 500 Myr (approximately the age of WW Cam), and 1 Gyr.

based on the effective temperatures are log $t = 8.703$ and log $t = 8.687$. There is reasonably good agreement between all these estimates, and the average evolutionary age for the system is log $t = 8.69$ (490 Myr).

Critical tests of evolutionary models in the sense defined by Andersen (1991) require the knowledge of the chemical abundance, in addition to the masses, radii, and temperatures, in order to provide tighter constraints on theory. Unfortunately, the observational determination of the overall metallicity of WW Cam is seriously complicated by the metallic-line nature of the binary. Our rough estimates mentioned earlier from photometry and spectroscopy are both higher than solar. However, this most likely represents only the surface layers of the stars and not the bulk metal abundance, which is the relevant quantity for the evolutionary calculations shown in Figure 6.

Among the eclipsing binaries with well-determined absolute dimensions, three have at least one component very similar in mass to the stars in WW Cam (which themselves differ by only 2.6%). The primary of RS Cha (Andersen 1975, 1991; Clausen & Nordström 1980) is essentially the same as WW Cam B (a difference of less than 0.8%, which is within the errors), as is the secondary of V624 Her (Popper 1984b; Andersen 1991) (different by only 0.5%). Both are somewhat more evolved than the secondary of WW Cam but also cooler by 200–300 K, in excellent agreement with expectations. As in the case of WW Cam, there are no observational determinations of the metallicity of RS Cha and V624 Her. Nevertheless, the consistency with the same tracks shown in Figure 6 may be taken as an indication that the abundance of those two systems, like that of WW Cam, cannot be far from solar. A third system, TZ For (Andersen et al. 1991), has a secondary with a mass about 1.5% larger than the primary of WW Cam but is much more evolved and 2000 K cooler. WW Cam is thus the least evolved of the well-observed systems in this mass regime.

Given the nonzero eccentricity we derive for the orbit of WW Cam ($e = 0.0098 \pm 0.0006$) despite the short period, it is of interest to compare this result with the predictions from tidal theory. We have computed the circularization time, as well as the times for synchronization of both components, using the radiative damping formalism by Zahn (1992 and references therein) as described by Claret & Cunha (1997). According to this theory, the orbit is not expected to become circular due to the action of tidal forces until an age of log $t = 9.154$. This is consistent with our measured eccentricity and the evolutionary age of log $t = 8.69$ we derived above. Synchronization of the components with the orbital motion is predicted to occur at log $t = 9.153$ for the primary and log $t = 9.155$ for the secondary. The v sin i values we measure are actually consistent with the stars' being already synchronized, within the errors (see Table 8). This appears to disagree with what is expected, although we cannot rule out that the small difference is real and that tidal forces are still adjusting the stars' rotation ever so slightly.

The hydrodynamic theory by Tassoul & Tassoul (1997 and references therein), also often used for comparisons with observations, predicts a time of circularization for WW Cam much shorter than the other tidal theory: log $t = 8.204$. In addition, the times of synchronization are 2 orders of magnitude shorter than before (log $t = 7.017$ for the primary and log $t = 7.018$ for the secondary). The hydrodynamic mechanism has often been found to be too efficient (e.g., Claret, Giménez, & Cunha 1995), but in this case our measured $v \sin i$ values seem to be consistent with the predictions, given the uncertainties. However, the time of circularization is clearly inconsistent with the fact that the orbit is eccentric.

Therefore, neither tidal theory is in complete agreement with the observations for WW Cam. A better evaluation of the synchronization aspect of the radiative clamping theory will require a more precise measure of the rotational velocities of the stars.

7. CONCLUSIONS

New photometric and spectroscopic observations of the eccentric eclipsing binary WW Cam combined with a reanalysis of data from the literature have allowed us to derive definitive orbital parameters and physical properties of the component stars. Our determinations have formal errors smaller than 1% in the masses and radii. WW Cam thus joins the elite of stars with the best measured absolute properties. At an age of about 500 million yr according to models, the system is still a relatively young main-sequence pair of stars with a high surface abundance of heavy elements compared with the solar composition. The two currently favored mechanisms that describe the tidal evolution of binary star properties disagree in their prediction of whether the rotation of the components of WW Cam should be synchronized with its orbital motion. Our own measurements of $v \sin i$ would seem to favor the hydrodynamic theory of Tassoul & Tassoul (1997) in this particular case. The remaining small eccentricity in the orbital motion of the system, however, is better explained by the radiative clamping theory by Zahn (1992), and is inconsistent with the other theory.

We thank P. Berlind, D. W. Latham, A. Milone, and R. P. Stefanik, who obtained many of the CfA spectrograms used here, and R. Davis, who maintains the CfA database of radial velocities. We are also grateful to Daryl Willmarth at KPNO for assistance with the spectroscopic observations there. This research has made use of the SIMBAD database, operated at the CDS, Strasbourg, France, and of NASA's Astrophysics Data System bibliographic services. This publication is partly supported by a grant to C. H. S. L. from the National Science Foundation.

REFERENCES

Agerer, F., & Hübscher, J. 1995, Inf. Bull. Variable Stars, No. 4222
Al-Naimiy, H. M. 1978, Ap&SS, 53, 181
Andersen, J. 1975, A&A, 44, 445
———. 1991, A&A Rev., 3, 91
Andersen, J., Clausen, J. V., Nordström, B., Tomkin, J., & Mayor, M. 1991, A&A, 246, 99
Braune, W. 1972, Inf. Bull. Variable Stars, No. 609
Braune, W., Hübscher, J., & Mundry, E. 1977, Astron. Nachr., 298, 121
Claret, A. 1995, A&AS, 109, 441
———. 1998, A&AS, 131, 395
Claret, A., & Cunha, N. C. S. 1997, A&A, 318, 187
Claret, A., & Giménez, A. 1992, A&AS, 96, 255
Claret, A., Giménez, A., & Cunha, N. C. S. 1995, A&A, 299, 724
Clausen, J. V., & Nordström, B. 1980, A&A, 83, 339
Crawford, D. L. 1979, AJ, 84, 1858 (erratum 85, 621 [1980])
Díaz-Cordovés, J., Claret, A., & Giménez, A. 1995, A&AS, 110, 329
Diethelm, R. 1972, BBSAG Bull., No. 5
———. 1974, BBSAG Bull., No. 17
———. 1975, BBSAG Bull., No. 19
Etzel, P. B. 1981, in Photometric and Spectroscopic Binary Systems, ed. E. B. Carling & Z. Kopal (NATO ASI Ser. C, 69) (Dordrecht: Reidel), 111
Fekel, F. C. 1999, in ASP Conf. Ser. 185, Precise Radial Velocities, ed. J. B. Hearnshaw & C. D. Scarfe (San Francisco: ASP), 378
Hayes, D. S. 1978, in IAU Symp. 80, The HR Diagram, ed. A. G. D. Philip & D. S. Hayes (Dordrecht: Reidel), 65
Hilditch, R. W., & Hill, G. 1975, MmRAS, 79, 101
Hoffleit, D., & Jaschek, C. 1982, The Bright Star Catalogue (4th rev. ed.; New Haven: Yale Univ. Obs.)
Huruhata, M., & Gaposchkin, S. 1940, Bull. Harvard Coll. Obs., 914, 11
Izotov, Yu. I., & Thuan, T. X. 1998, ApJ, 500, 188
Kundera, T. 2001, Eclipsing Binaries Minima Database (Kraków: Obs. Astron. Uniw. Jagiellońksiego)
Lacy, C. H. 1984, Inf. Bull. Variable Stars, No. 2489 (erratum No. 2523)
Lacy, C. H. S. 1992, AJ, 104, 801
———. 2002, in preparation
Lacy, C. H. S., Clem, J. L., Zakirov, M., Arzumanyants, G. C., Bairamov, N. R., & Hojaev, A. S. 1998, Inf. Bull. Variable Stars, No. 4597
Lacy, C. H. S., Hood, B., & Straughn, A. 2001, Inf. Bull. Variable Stars, No. 5067
Lacy, C. H. S., Marcrum, K., & İbanoğlu, C. 1999, Inf. Bull. Variable Stars, No. 4737
Latham, D. W. 1992, in IAU Colloq. 135, Complementary Approaches to Double and Multiple Star Research, ed. H. A. McAlister & W. I. Hartkopf (ASP Conf. Ser. 32) (San Francisco: ASP), 110
Nelson, R. H. 2001, Inf. Bull. Variable Stars, No. 5040
Pagel, B. E. J., & Portinari, L. 1998, MNRAS, 298, 747
Peimbert, M. 1993, Rev. Mexicana Astron. Astrofis., 27, 9
Peter, H. 1972a, BBSAG Bull., No. 3
———. 1972b, BBSAG Bull., No. 6
Popper, D. M. 1980, ARA&A, 18, 115
———. 1984a, AJ, 89, 132
———. 1984b, AJ, 89, 1057
Popper, D. M., & Etzel, P. B. 1981, AJ, 86, 102
Stefanik, R. P., Latham, D. W., & Torres, G. 1999, in IAU Colloq. 170, Precise Stellar Radial Velocities, ed. J. B. Hernshaw & C. D. Scarfe (ASP Conf. Ser. 185) (San Francisco: ASP), 354
Strömgren, B. 1966, ARA&A, 4, 433
Tassoul, M., & Tassoul, J.-L. 1997, ApJ, 481, 363
Torres, G., Lacy, C. H. S., Claret, A., & Sabby, J. A. 2000, AJ, 120, 3226
von Zschocke, W. 1974, Mitt. Veränderl. Sterne, 6, 93
Wade, R. A., & Rucinski, S. M. 1985, A&AS, 60, 471
Zahn, J.-P. 1992, in Binaries as Tracers of Stellar Formation, ed. A. Duquennoy & M. Mayor (Cambridge: Cambridge Univ. Press), 253
Zucker, S., & Mazeh, T. 1994, ApJ, 420, 806